Biogeosciences, 17, 3891–3901, 2020
https://doi.org/10.5194/bg-17-3891-2020

Biogeosciences Open Access EGU

The stable carbon isotope signature of methane produced by saprotrophic fungi

Moritz Schroll[1], Frank Keppler[1,2], Markus Greule[1], Christian Eckhardt[3], Holger Zorn[4], and Katharina Lenhart[5,6]

[1]Institute of Earth Sciences, Heidelberg University, Im Neuenheimer Feld 236, 69120 Heidelberg, Germany
[2]Heidelberg Center for the Environment (HCE), Heidelberg University, Im Neuenheimer Feld 229, 69120 Heidelberg, Germany
[3]Department of Plant Ecology, Justus Liebig University Giessen, IFZ, 26–32, 35392 Giessen, Germany
[4]Institute of Food Chemistry and Food Biotechnology, Justus Liebig University Giessen, IFZ, 58, 35392 Giessen, Germany
[5]Centre for Organismal Studies (COS), Im Neuenheimer Feld 230, 69120 Heidelberg, Germany
[6]Bingen University of Applied Sciences, Berlinstraße 109, 55411 Bingen, Germany

Correspondence: Moritz Schroll (moritz.schroll@geow.uni-heidelberg.de) and Katharina Lenhart (k.lenhart@th-bingen.de)

Received: 25 March 2020 – Discussion started: 2 April 2020
Revised: 9 June 2020 – Accepted: 24 June 2020 – Published: 31 July 2020

Abstract. Methane (CH_4) is the most abundant organic compound in the atmosphere and is emitted from many biotic and abiotic sources. Recent studies have shown that CH_4 production occurs under aerobic conditions in eukaryotes, such as plants, animals, algae, and saprotrophic fungi. Saprotrophic fungi play an important role in nutrient recycling in terrestrial ecosystems via the decomposition of plant litter. Although CH_4 production by saprotrophic fungi has been reported, no data on the stable carbon isotope values of the emitted CH_4 (δ^{13}C-CH_4 values) are currently available. In this study, we measured the δ^{13}C values of CH_4 and carbon dioxide (δ^{13}C-CO_2 values) emitted by two saprotrophic fungi, *Pleurotus sapidus* (oyster mushroom) and *Laetiporus sulphureus* (sulphur shelf), cultivated on three different substrates, pine wood (*Pinus sylvestris*), grass (mixture of *Lolium perenne*, *Poa pratensis*, and *Festuca rubra*), and corn (*Zea mays*), which reflect both C_3 and C_4 plants with distinguished bulk δ^{13}C values. Applying Keeling plots, we found that the δ^{13}C source values of CH_4 emitted from fungi cover a wide range from −40 to −69 mUr depending on the growth substrate and fungal species. Whilst little apparent carbon isotopic fractionation (in the range from −0.3 to 4.6 mUr) was calculated for the δ^{13}C values of CO_2 released from *P. sapidus* and *L. sulphureus* relative to the bulk δ^{13}C values of the growth substrates, much larger carbon isotopic fractionations (ranging from −22 to −42 mUr) were observed for the formation of CH_4. Although the two fungal species showed similar $\delta^{13}CH_4$ source values when grown on pine wood, $\delta^{13}CH_4$ source values differed substantially between the two fungal species when they were grown on grass or corn. We found that the source values of $\delta^{13}CH_4$ emitted by saprotrophic fungi are highly dependent on the fungal species and the metabolized substrate. The source values of $\delta^{13}CH_4$ cover a broad range and overlap with values reported for methanogenic archaea, the thermogenic degradation of organic matter, and other eukaryotes.

1 Introduction

Methane (CH_4) is an important greenhouse gas that is emitted by several abiotic sources (e.g. fossil fuel, biomass burning, and geological processes) and biotic sources (e.g. wetlands, agriculture and waste, and fresh waters) to the atmosphere (Kirschke et al., 2013; Saunois et al., 2016, 2020). In the past, biotic CH_4 production has been attributed exclusively to strictly anaerobic microorganisms, such as methanogens, that are ubiquitous in wetlands, rice paddies, landfills, and the intestines of termites and ruminants (Kirschke et al., 2013). The discovery of CH_4 emissions from dead and living plants under oxic conditions (Keppler et al., 2006, 2009) paved the way for the search for new biogenic CH_4 sources. Since then, several previously unknown CH_4 sources have been discovered, including the endothelial cells

of rat liver (Boros and Keppler, 2019; Ghyczy et al., 2008), plant cell cultures (Wishkerman et al., 2011), marine algae (Klintzsch et al., 2019; Lenhart et al., 2016), marine and terrestrial cyanobacteria (Bižić et al., 2020), humans (Keppler et al., 2016), and saprotrophic fungi (Lenhart et al., 2012).

Fungi play a central role in ecosystems by decomposing organic matter, thereby recycling formerly bound carbon and nutrients (Grinhut et al., 2007). This process is especially important in forests where fungi are essential for wood decay and have a great impact on the carbon and nitrogen cycles (Ralph and Catcheside, 2002). White rot fungi (e.g. *Trametes versicolor* or *Pleurotus ostreatus*) are able to decompose the chemically complex structural component lignin, whereas brown rot fungi (e.g. *Serpula lacrymans* or *Gloeophyllum trabeum*) mainly metabolize cellulose and hemicellulose (Ten Have and Teunissen, 2001; Leonowicz et al., 1999; Valášková and Baldrian, 2006). Fungi have already been determined to be involved in the synthesis of CH_4 during wood decay (Beckmann et al., 2011; Mukhin and Voronin, 2007, 2008) via the breakdown of large macromolecules to smaller molecules, thereby providing bacteria and archaea with essential substrate. Elevated levels of CH_4 were found in fungus-infected wood stems with oxygen concentrations ranging from 1 % to 14 % (Hietala et al., 2015). Here, CH_4 production was associated with anoxic microsites in the xylem, indicating that at least part of the CH_4 was produced by methanogenic archaea. Nevertheless, Lenhart et al., 2012 demonstrated that basidiomycetes are able to produce CH_4 under aerobic conditions without the presence of methanogenic archaea. Therefore, fungi might be an underestimated source of CH_4 in the global CH_4 cycle.

Stable carbon isotopes (expressed as $\delta^{13}C$ values) have often been used to investigate sources and sinks of CH_4 on the global scale (Whiticar, 1993). As different CH_4 sources have characteristic $\delta^{13}C$ values, $\delta^{13}C$-CH_4 values might be used to quantify the individual contributions of various sources regionally and/or globally (Dlugokencky et al., 2011; Hein et al., 1997; Nisbet et al., 2016; Quay et al., 1999; Tyler, 1986; Whiticar, 1999). The short lifetime of CH_4 in the atmosphere (from 9.7 ± 1.5 to 11.2 ± 1.3 years; Naik et al., 2013; Prather et al., 2012; Voulgarakis et al., 2013) assures that global isotopic $\delta^{13}C$-CH_4 patterns represent the average of recent inputs by various sources and allows for the quantification of respective source strengths (Mikaloff Fletcher et al., 2004a, b).

Additionally, stable isotopes provide information about the formation processes of CH_4. Traditionally, three formation categories of $\delta^{13}C$-CH_4 values have been identified: biogenic, with typical $\delta^{13}C$-CH_4 values ranging from ~ -55 to -70 mUr; thermogenic, with typical $\delta^{13}C$-CH_4 values ranging from ~ -25 to -55 mUr; and pyrogenic, with typical $\delta^{13}C$-CH_4 values ranging from ~ -13 to -25 mUr (Kirschke et al., 2013). However, stable isotope values of recently identified CH_4 sources, i.e. human CH_4 emissions (-56 to -95 mUr; Keppler et al., 2016), plant-derived CH_4 (-52 to -69 mUr; Keppler et al., 2006), and abiotic UV-induced CH_4 formation by plants (-52 to -67 mUr; Vigano et al., 2009) also need to be considered.

In this study, we investigated the stable carbon isotope source signatures of CH_4 and CO_2 released by the two basidiomycetes *Pleurotus sapidus* (white rot fungus) and *Laetiporus sulphureus* (brown rot fungus). Both fungi were cultivated under sterile conditions on three different substrates (pine wood, grass, and corn) with varying bulk $\delta^{13}C$ values. We examined the influence of fungal species and growth substrate on $\delta^{13}C$-CH_4 and $\delta^{13}C$-CO_2 values and compared the $\delta^{13}C$-CH_4 values from the two fungal species with those of other known sources reported in the literature.

2 Material and methods

2.1 Selected fungi

P. sapidus (Pleurotaceae, DSMZ 8266) and *L. sulphureus* (Polyporacaeae, DSMZ 1014) were chosen for this experiment because of their capability to emit CH_4 (Lenhart et al., 2012), their ecological and physiological characteristics (*P. sapidus* is a white rot fungus and *L. sulphureus* is a brown rot fungus), and their well-established practical handling under laboratory conditions.

2.2 Cultivation of fungi and incubation experiments

Pine wood (*Pinus sylvestris*), grass (mixture of *Lolium perenne*, *Poa pratensis*, and *Festuca rubra*) and corn (*Zea mays*) were selected as growth substrates. Pine wood was chosen to investigate if white rot and brown rot fungi differ with respect to the $\delta^{13}C$-CH_4 and $\delta^{13}C$-CO_2 values released during wood decay. Therefore, dead pine wood branches were collected from the forest floor and shredded to small wood chips with a length of about 5 cm (Natura 1800L; Gloria, Witten, Germany). The wood chips were dried at 60 °C for 48 h and stored in a flask (WECK GmbH, Hanau, Germany). Grass (C_3 plant) and corn (C_4 plant) were selected because of their different stable isotope values. As the metabolic pathway for carbon fixation is biochemically different in C_3 and C_4 plants, plant biomass differs with respect to $\delta^{13}C$ values, which, in turn, might lead to different $\delta^{13}C$ values of CH_4 and CO_2 released by fungi. Therefore, typical garden lawn was manually cut, dried at 70 °C, and stored in a flask. The corn substrate consisted of conventional corn flour.

The substrates were autoclaved, filled into 2.7 L flasks (WECK GmbH, Hanau, Germany), and inoculated with pure fungal submerged cultures under sterile conditions following Lenhart et al. (2012). After the addition of the fungi, the flasks were closed with lids and a rubber band sealing. To allow gas exchange during the fungal growth period (about 2 weeks), a hole in the centre of every lid was fitted with a cotton stopper. Before the start of the incubation experi-

ments, the flasks were aerated under sterile conditions in order to start the incubation at atmospheric CH_4 mixing ratios. Additionally, to create an airtight seal, the flask's cotton stoppers were replaced by sterile silicone stoppers (Saint-Gobain Performance Plastics, Charny, France).

For the incubation experiments, *P. sapidus* and *L. sulphureus* were incubated on the three substrates, while uninoculated substrates were also incubated as control treatments. Before the incubation experiments, the substrates were sterilized by autoclaving at 121 °C and 2 bar pressure for 20 min. The incubation experiments were conducted using three replicates per treatment. The duration of the incubation accounted for up to 40 h. All incubations were conducted at room temperature (23 ± 1.5 °C). At every sampling point, 40 mL of air was taken from the flasks for gas concentration measurements and an additional 40 mL was taken for δ^{13}C-CH_4 stable isotope ratio mass spectrometry (IRMS) analysis. The gas samples were taken with airtight 60 mL PE syringes (Plastipak, BD, Franklin Lakes, USA) and transferred into 12 mL evacuated Exetainer vials (Labco, High Wycombe, UK). Subsequently, a volume of atmospheric air equivalent to the volume of the removed sample was added into each flask directly after sampling. Mixing ratios and stable isotope values of CH_4 were corrected according to the dilution.

When calculating the fungal CH_4 and CO_2 production rates, we subtracted substrate-derived CH_4 and CO_2 production rates (determined using the control treatments) from the respective fungi-containing samples. Additionally, only sample points showing a linear increase in CH_4 and CO_2 were considered in the calculation of the fungal production rates.

To account for differences in the metabolic activity of the fungi, we additionally measured respiration rates, assuming that metabolic activity correlates with respiration and, therefore, the CO_2 emissions of the fungi. Hence, we related fungus-derived CH_4 emissions to respiration by calculating the $CH_4 : CO_2$ emission ratio.

2.3 Analysis of CH_4 and CO_2 via gas chromatography

Samples were analysed using a gas chromatograph (GC, Bruker Greenhouse Gas Analyser 450-GC) equipped with a flame ionization detector (FID) and an electron capture detector (ECD) for the detection of CH_4 and CO_2 respectively. The detector temperatures were set at 300 °C (FID) and 350 °C (ECD). Five reference gases (Deuste Steininger GmbH) were used to calibrate the GC system. The reference gases were in the range from 1 ppmv (parts per million by volume) to 21 and from 304 to 40 000 ppmv for CH_4 and CO_2 respectively. Gas peaks were integrated using Galaxie software (Varian Inc., Palo Alto, CA, USA).

2.4 Definition of δ values and isotope apparent fractionation

In this paper, all stable carbon isotope ratios are expressed in the conventional "delta" (δ) notation, meaning the relative difference of the isotope ratio of a substance from the standard substance Vienna Peedee Belemnite (V-PDB):

$$\delta^{13}\mathrm{C} = \frac{\left(\frac{^{13}\mathrm{C}}{^{12}\mathrm{C}}\right)_{\mathrm{sample}}}{\left(\frac{^{13}\mathrm{C}}{^{12}\mathrm{C}}\right)_{\mathrm{V\text{-}PDB}}} - 1 \quad (1)$$

The apparent fractionation ($\varepsilon_{\mathrm{app}}$) between fungal δ^{13}C-CH_4 or δ^{13}C-CO_2 values and the δ^{13}C values of the substrates was calculated according to Eq. (2):

$$\varepsilon_{\mathrm{app}}\ CH_4 \text{ or } CO_2 = \frac{(\delta^{13}\mathrm{C}+1)_{\mathrm{fungal\ CH_4\ or\ CO_2}}}{(\delta^{13}\mathrm{C}+1)_{\mathrm{substrate}}} - 1 \quad (2)$$

We follow the proposal of Brand and Coplen (2012) and use the term "urey" (Ur) as the isotope delta unit, in order to conform with the guidelines for the International System of Units (SI). Hence, isotope delta values that were formerly given as −70 ‰ are expressed as −70 mUr.

2.5 Measurements of $\delta^{13}CH_4$ and $\delta^{13}CO_2$ values

Stable carbon isotope values of CH_4 and CO_2 were measured using a continuous flow isotope mass spectrometry system (CF-IRMS). A HP 6890N GC (Agilent, Santa Clara, USA) was linked to a pre-concentration unit for CH_4 measurements and an A200S autosampler (CTC Analytics, Zwingen, Switzerland) for CO_2 analysis. The GC was equipped with a CP-PoraPLOT Q capillary column (27.5 m × 0.25 mm i.d., film thickness 8 µm; Varian, Palo Alto, USA). The GC was operated with an injector temperature of 200 °C, an isothermal oven temperature of 30 °C, split injection (10 : 1), and a constant carrier gas flow of 1.8 mL min^{-1} (methane-free helium). The GC was coupled to a Delta$^{\mathrm{PLUS}}$XL isotope ratio mass spectrometer (ThermoQuest Finnigan, Bremen, Germany) via an oxidation reactor and a GC Combustion III interface (ThermoQuest Finnigan, Bremen, Germany). The oxidation reactor was employed with the following properties: a ceramic tube (Al_2O_3; length 320 mm, 1.0 mm i.d.) with Ni/Pt wires inside activated by oxygen and a reactor temperature of 960 °C.

For CH_4 measurements with the pre-concentration unit, headspace gas samples were transferred to an evacuated 40 mL sample loop. Methane was trapped on HayeSep D, separated from other compounds by the GC, and then introduced into the IRMS system via an open split. The monitor gas was carbon dioxide of high purity (carbon dioxide 4.5, Messer Griesheim, Frankfurt, Germany) with a known δ^{13}C value of −23.6 mUr (calibrated at the Max Planck Institute for Biogeochemistry in Jena, Germany). All δ^{13}C values were corrected using two CH_4 reference standards (Isometric instruments, Victoria, Canada) with δ^{13}C values of

−23.9±0.2 and −54.5±0.2 mUr that were calibrated against International Atomic Energy Agency (IAEA) and National Institute of Standards and Technology (NIST) reference substances. The normalization of the sample values was carried out according to Paul et al. (2007).

2.6 Bulk isotope analysis of fungal substrates

Stable carbon isotope values of the bulk substrate were measured using an FlashEA 1112 elemental analyser (Thermo Fisher Scientific, Germany) coupled to a Delta V IRMS (Thermo Fisher Scientific, Germany). Therefore, 0.06 mg of the substrate was put into a tin cup and combusted in the elemental analyser. The resulting gases were separated in a GC by a CP-PoraPLOT Q capillary column (27.5 m × 0.25 mm i.d., film thickness 8 µm; Varian, Palo Alto, USA) and then reached the Delta V IRMS via a Conflo IV universal continuous flow interface (Thermo Fisher Scientific, Germany). Isotope values were corrected using USGS 40 and USGS 41 standards.

2.7 Determination of isotopic source signature of CH_4 and CO_2 applying Keeling plots

For the determination of $\delta^{13}C$ source values of CH_4 and CO_2, the Keeling plot method was used (Keeling, 1958; Pataki et al., 2003):

$$\delta^{13}C_a = c_b\left(\delta^{13}C_b - \delta^{13}C_s\right)\left(\frac{1}{c_a}\right) + \delta^{13}C_s, \quad (3)$$

where c_a is the mixing ratio of CH_4/CO_2 in the headspace, $\delta^{13}C_a$ is the $\delta^{13}C$ value of CH_4/CO_2 in the headspace, c_b is the mixing ratio of background CH_4/CO_2, $\delta^{13}C_b$ is the $\delta^{13}C$ value of background CH_4/CO_2, and $\delta^{13}C_s$ is the $\delta^{13}C$ source value of the CH_4/CO_2. For a more detailed description of the application of Keeling plots for the determination of the CH_4 source signature, we refer to the study by Keppler et al. (2016).

$\delta^{13}C$-CH_4 source signatures were calculated following the Keeling plot method for each flask. Results of the Keeling plots are then given as the arithmetic mean of the three individual flasks per treatment with their standard deviations ($n = 3$).

The $\delta^{13}C$-CH_4 source signatures of each flask of *P. sapidus* and *L. sulphureus* grown on pine were corrected for CH_4 emissions and $\delta^{13}C$-CH_4 values of the "pine" control samples using the following mass balance approach:

$$\delta^{13}C_{\text{fungi corrected}} = \frac{\left(P(CH_4)_{\text{fungi}} \cdot \delta^{13}C_{\text{fungi}}\right) - \left(P(CH_4)_{\text{pine}} \cdot \delta^{13}C_{\text{pine}}\right)}{\left(P(CH_4)_{\text{fungi}} - P(CH_4)_{\text{pine}}\right)}, \quad (4)$$

where $P(CH_4)_{\text{fungi/pine wood}}$ is the CH_4 emitted by the fungi or pine wood, and $\delta^{13}C_{\text{fungi/pinewood}}$ is the $\delta^{13}C$-CH_4 source signature of the fungi or pine wood derived from the Keeling plots. Corrected $\delta^{13}C$-CH_4 source values for *P. sapidus* and *L. sulphureus* are given as the arithmetic mean of the three individual flasks per treatment with their standard deviations ($n = 3$).

The determination coefficient (R^2) of the Keeling plots showed values higher than 0.93 except for *P. sapidus* grown on grass ($R^2 = 0.51$). The lower R^2 value for *P. sapidus* grown on grass is probably a result of the marginal changes in the $\delta^{13}C$-CH_4 values due to the small increase in the CH_4 mixing ratio compared with the background CH_4 mixing ratio. Therefore, the low R^2 does not necessarily indicate a weaker relationship between the CH_4 mixing ratio and the $\delta^{13}C$-CH_4 value.

2.8 Statistics

Mixing ratios and production rates of CH_4, CO_2, $\delta^{13}C$-CH_4 values, and $\delta^{13}C$-CO_2 values as well as $\delta^{13}C$ source values are presented as the arithmetic mean of three independent replicates with their standard deviations ($n = 3$). Linear regression analysis, the arithmetic means, and their standard deviations were calculated using Microsoft Excel (Microsoft Excel for Office 365 MSO). Two-way analysis of variance (ANOVA) tests (SigmaPlot 12.2.0.45, USA) were carried out to test for species- and substrate-related effects on the $\delta^{13}C$-CH_4 and $\delta^{13}C$-CO_2 source values for each treatment. Differences at the $p < 0.05$ level were referred to as significant.

3 Results and discussion

In this section, we firstly present the results of CH_4 and CO_2 production from the two fungal species grown on the three different substrates. This includes emission rates of CH_4 and CO_2 from the control treatments of pine wood, grass, and corn as well as the molar ratio of CH_4 and CO_2. Secondly, we then present the respective stable isotope values measured for CH_4 and CO_2 during the incubation experiments and calculate the stable isotope source values of CH_4 and CO_2 released by the fungi applying Keeling plots. We then compare these values with stable carbon isotope values of the bulk organic matter by calculating the apparent fractionation. Finally, we compare $\delta^{13}C$ source values of fungus-derived CH_4 with known values for other CH_4 sources from the literature.

3.1 Release of CH_4 and CO_2 from *P. sapidus* and *L. sulphureus*

All incubation experiments in which fungi were grown on different substrates showed a significant increase in CH_4 compared with the respective substrate control (Fig. 1a, c). Calculated emission rates for CH_4 and CO_2 are presented in Table 1. *L. sulphureus* grown on grass (7.5 ± 1.3 nmol h^{-1}) showed the highest emission rate of CH_4, followed by *L. sulphureus* grown on pine (6.2 ± 0.3 nmol h^{-1}), *P. sapidus* grown on corn (4.4 ± 1.9 nmol h^{-1}), *L. sulphureus* grown

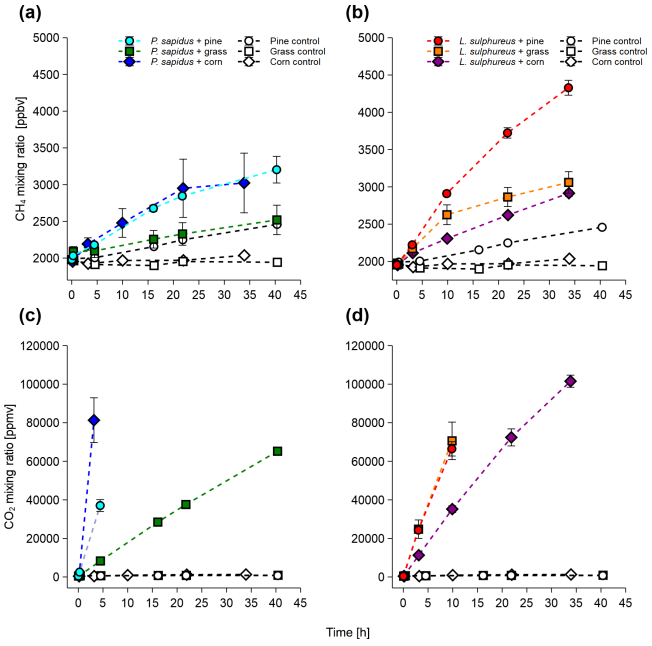

Figure 1. Mixing ratios of CH_4 and CO_2 of *P. sapidus* **(a, c)** and *L. sulphureus* **(b, d)** grown on pine wood, grass, and corn. Mixing ratios are presented as mean values with their standard deviation ($n = 3$).

on corn (2.6 ± 0.1 nmol h^{-1}), *P. sapidus* grown on pine (2.5 ± 0.2 nmol h^{-1}), and *P. sapidus* grown on grass (1.4 ± 0.5 nmol h^{-1}). Please note that CH_4 and CO_2 emission rates are not related to fungal biomass. Therefore, differences in the emission rates might be due to varying fungal biomass of the subsamples. Instead, CH_4 production was related to CO_2 production by determining the molar emission ratio between CH_4 and CO_2 (µmol CH_4 : mol CO_2). Thus, CO_2 production reflects the amount of fungal biomass and is also an indicator of the metabolic activity of the fungi.

The control flasks did not show significant changes in their CH_4 and CO_2 mixing ratios over time, except for CH_4 in pine wood controls (1.3 ± 0.1 nmol h^{-1}). However, small CH_4 emission rates of 0.25 ± 0.01 nmol h^{-1} were observed in the control flasks of corn, and the CH_4 mixing ratio slightly decreased over time in the grass control (-0.05 ± 0.04 nmol h^{-1}). Whilst the pine wood and corn control flasks showed a small increase in the CH_4 mixing ratio, they did not show an increase in the CO_2 mixing ratios. These data rule out contamination by microbial heterotrophs, as this would cause a measurable CO_2 increase within the flasks. The CH_4 increase in the substrate controls might be attributed to CH_4 release by dead plant material, as was already shown by Keppler et al. (2006) and Vigano et al. (2009). Within the scope of these experiments, no analytic test for microbial contamination was conducted. Nevertheless, using three different methods (fluorescence in situ hybridization, FISH; confocal laser scanning microscopy, CLSM; and quantitative real-time polymerase chain reaction), Lenhart et al. (2012) clearly showed that no methanogenic archaea were present in the same method of cultivation of fungi and incubation experiments that were performed in this study. Furthermore, CH_4 and CO_2 release and the $CH_4 : CO_2$ emission ratios in our incubations are similar to the experiments of Lenhart et al. (2012) and do not indicate microbial contamination. Therefore, we assume that no contamination with bacteria or methanogenic archaea was present in our investigations.

For *P. sapidus* grown on corn and *L. sulphureus* grown on grass, no further linear increase in CH_4 was observed after 22 and 10 h respectively. This might be due to the reduced decay of organic matter and slower fungal metabolism owing to higher CO_2 and lower O_2 mixing ratios.

A drastic increase in CO_2 mixing ratios relative to the controls was observed in all flasks containing fungi (Fig. 1b, d). The CO_2 emission rates are shown in Table 1. CO_2 production rates ranged from 176 ± 4 to 2910 ± 410 µmol h^{-1} for *P. sapidus* grown on grass and *P. sapidus* grown on corn respectively. These highly variable CO_2 production rates might reflect different fungal biomass and metabolic activity (mineralization of organic matter). In the control treatments, tiny increases in the CO_2 mixing ratio were detected ranging from 0.64 ± 0.12 to 0.91 ± 0.14 µmol h^{-1}. Only one flask (corn control) showed a somewhat higher increase in CO_2 (7.76 µmol h^{-1}), which was most likely caused by microbial contamination of the flask. However, no increase in the CH_4 mixing ratio was detected (see Supplement). Therefore, this control flask was excluded from further calculations.

Mean CH_4 and CO_2 emission rates and $CH_4 : CO_2$ emission ratios of all treatments are presented in Table 1. Higher ratios indicate a higher CH_4 production during decay of the substrates. Therefore, both fungal species and substrate affect the $CH_4 : CO_2$ emission ratio ($p < 0.001$). For *P. sapidus*, $CH_4 : CO_2$ emission ratios are more variable (1.4 to 8.0 µmol CH_4/mol CO_2) compared with *L. sulphureus* (6.7–9.6 µmol CH_4/mol CO_2). This variation might be due to differences in the fungi's enzyme sets required for organic matter decay, as *P. sapidus* is a white rot fungus and *L. sulphureus* is a brown rot fungus. At present, the biochemical pathways that lead to CH_4 are still unknown, although compounds such as the sulfur-bound methyl-group of methionine and glucose have been identified to act as carbon precursors of fungus-derived CH_4 (Lenhart et al., 2012).

Lenhart et al., 2012 found CH_4 : CO_2 ratios of fungi that ranged between 8 µmol CH_4/mol CO_2 and 17 µmol CH_4/mol CO_2, which is in the same order of magnitude as the $CH_4 : CO_2$ ratios determined in this study. It should be noted that, for better comparability, the $CH_4 : CO_2$ ratios of Lenhart et al. (2012; given in ppbv CH_4 : % CO_2) were converted to fit the $CH_4 : CO_2$ ratio units used in this study (µmol CH_4 : mol CO_2).

Table 1. CH_4 and CO_2 production rates and molar $CH_4 : CO_2$ emission ratios of the fungi incubated on different substrates. Values are presented as mean values of three independent replicates with their standard deviation ($n = 3$), except for the control "corn" ($n = 2$).

Fungi	Substrate	CH_4 production rate ($nmol\,h^{-1}$)	CO_2 production rate ($\mu mol\,h^{-1}$)	$CH_4 : CO_2$ ratio ($\mu mol\,mol^{-1}$)
P. sapidus	Pine	2.5 ± 0.2	901 ± 79	2.8 ± 0.4
	Grass	1.4 ± 0.5	176 ± 4	8.0 ± 2.8
	Corn	4.4 ± 1.9	2910 ± 419	1.4 ± 0.5
L. sulphureus	Pine	6.2 ± 0.3	724 ± 42	8.6 ± 1.0
	Grass	7.5 ± 1.3	771 ± 103	9.6 ± 0.5
	Corn	2.6 ± 0.1	385 ± 20	6.7 ± 0.4
Control	Pine	1.3 ± 0.1	0.64 ± 0.12	–
	Grass	-0.05 ± 0.04	0.91 ± 0.14	–
	Corn	0.25	0.66	–

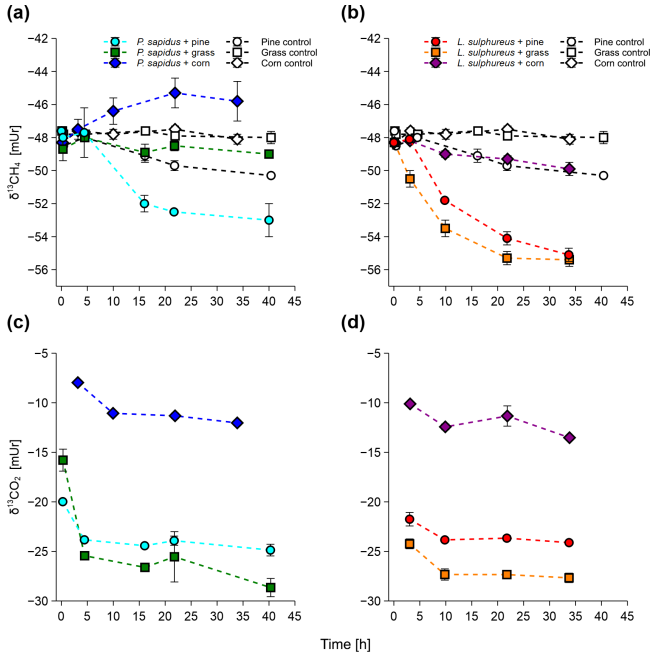

Figure 2. Stable carbon isotope values of CH_4 and CO_2 of *P. sapidus* **(a, c)** and *L. sulphureus* **(b, d)** grown on pine, grass, and corn. Values are presented as mean values with their standard deviation ($n = 3$), except for $\delta^{13}CO_2$ values of *L. sulphureus* grown on corn ($n = 2$).

3.2 Stable carbon isotope values of CH_4 and CO_2

Stable carbon isotope values of CH_4 and CO_2 measured from the incubation experiments are presented in Fig. 2. All incubations show a trend towards more negative δ^{13}C-CH_4 values (less ^{13}C) with time except for *P. sapidus* grown on corn, where a tendency towards more positive δ^{13}C-CH_4 values was observed (Fig. 2a, b). During the incubation, δ^{13}C-CH_4 values changed from -47.7 ± 0.1 mUr (for the incubation of *P. sapidus* grown on pine/grass) and -48.2 ± 0.1 mUr (for the incubation of *P. sapidus* grown on corn and *L. sulphureus* grown on pine/grass/corn) to -53.0 ± 0.7 mUr (for *P. sapidus* grown on pine), -48.7 ± 0.3 mUr (for *P. sapidus* grown on grass), -45.8 ± 1.2 mUr (for *P. sapidus* grown on corn), -55.1 ± 0.4 mUr (for *L. sulphureus* grown on pine), -55.4 ± 0.4 mUr (for *L. sulphureus* grown on grass), and -49.9 ± 0.4 mUr (for *L. sulphureus* grown on corn). The controls showed no significant shift in δ^{13}C-CH_4 values except for the pine control, where an increase in the CH_4 mixing ratio along with more negative values of δ^{13}C-CH_4 values occurred over time. This was accounted for when calculating the δ^{13}C-CH_4 source signatures for *P. sapidus* grown on pine and *L. sulphureus* grown on pine (see Sect. 2.7).

The δ^{13}C-CO_2 values showed a trend towards more negative values within the first 3–4 h of incubation (Fig. 2c, d). After this time, only minor changes in the δ^{13}C-CO_2 values occurred. Final δ^{13}C-CO_2 values of the incubation were -24.9 ± 0.6 mUr (for *P. sapidus* grown on pine), -28.6 ± 0.9 mUr (for *P. sapidus* grown on grass), -12.0 ± 0.3 mUr (for *P. sapidus* grown on corn), -24.1 ± 0.1 mUr (for *L. sulphureus* grown on pine), -27.7 ± 0.5 mUr (for *L. sulphureus* grown on grass), and -13.0 ± 0.5 mUr (for *L. sulphureus* grown on corn).

3.3 δ^{13}C-CH_4 and δ^{13}C-CO_2 source signatures of fungi

The δ^{13}C-CH_4 source signatures determined via a Keeling plot analysis (Fig. 3) that ranged from -69.2 ± 1.9 mUr (for *L. sulphureus* grown on grass) to -39.8 ± 2.0 mUr (for *P. sapidus* grown on corn) are presented in Table 2. Average δ^{13}C-CH_4 source signatures for each fungal species, considering all three substrates, are -52.6 mUr for *P. sapidus* and -61.3 mUr for *L. sulphureus*. These results suggest that the fungal species significantly influence the isotopic values of the emitted CH_4 ($p < 0.001$). A possible explanation for this observation could be the different enzyme sets of both fungi that decompose different components of the growth substrates, as *P. sapidus* belongs to white rot fungi and *L.*

Table 2. Calculated δ^{13}C-CH_4 and δ^{13}C-CO_2 source signatures, δ^{13}C values of the substrates, and $\varepsilon_{app\ CH_4}$ and $\varepsilon_{app\ CO_2}$. Values are presented as mean values with their standard deviation ($n = 3$).

Fungi	Substrate	δ^{13}C-CH_4 source (mUr)	δ^{13}C-CO_2 source (mUr)	δ^{13}C substrate (mUr)	$\varepsilon_{app\ CH_4}$ (mUr)	$\varepsilon_{app\ CO_2}$ (mUr)
P. sapidus	Pine	-65.3 ± 1.1	-24.1 ± 0.1		-38.4 ± 1.2	4.0 ± 0.1
	Grass	-52.9 ± 1.6	-27.4 ± 1.3		-21.8 ± 1.7	4.6 ± 1.3
	Corn	-39.8 ± 2.0	-12.0 ± 0.3		-28.5 ± 2.0	-0.3 ± 0.3
L. sulphureus	Pine	-61.4 ± 0.5	-25.0 ± 0.5		-34.4 ± 0.6	3.0 ± 0.4
	Grass	-69.2 ± 1.9	-29.0 ± 0.5		-38.6 ± 2.0	2.9 ± 0.5
	Corn	-53.4 ± 1.1	-12.8 ± 0.3		-42.2 ± 1.1	-1.1 ± 0.3
Control	Pine			-28.0 ± 0.5		
	Grass			-31.5 ± 0.6		
	Corn			-11.7 ± 0.1		

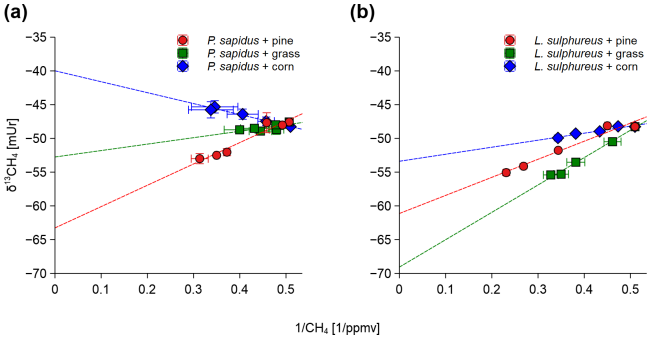

Figure 3. Keeling plots shown for *P. sapidus* **(a)** and *L. sulphureus* **(b)** grown on the three substrates. Sample points in the graphs are given as the arithmetic mean of the δ^{13}C-CH_4 or δ^{13}C-CO_2 values with their standard deviation ($n = 3$) on the y axis and the arithmetic mean of the inverted mixing ratio of CH_4 or CO_2 with their standard deviation ($n = 3$) on the x axis.

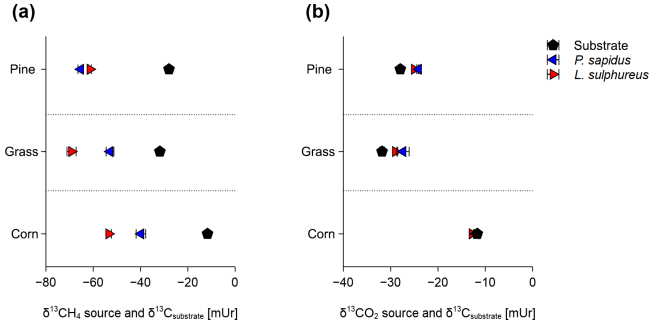

Figure 4. Calculated source signatures of δ^{13}C-CH_4 values **(a)** and δ^{13}C-CO_2 values **(b)** from *P. sapidus*, *L. sulphureus* as well as the δ^{13}C values of the substrate. The data points represent the mean values of the individual Keeling plots with their standard deviation ($n = 3$).

sulphureus is a brown rot fungus. However, detailed investigations of the metabolic pathways leading to CH_4 formation were beyond the scope of this study.

Furthermore, a significant effect of the growth substrate on δ^{13}C-CH_4 source signatures was observed ($p < 0.001$). δ^{13}C-CH_4 source signatures from *P. sapidus* were more positive compared with those of *L. sulphureus* when grown on grass ($\Delta = 16.3$ mUr) and corn ($\Delta = 13.6$ mUr) (Fig. 4). When grown on pine wood, δ^{13}C-CH_4 source signatures were similar, with *P. sapidus* showing slightly more negative values ($\Delta = -3.9$ mUr). Methane emitted by both fungi grown on corn was generally more enriched in ^{13}C (less negative δ^{13}C-CH_4 source values) compared with the fungi grown on pine wood and grass. This might be easily explained by the δ^{13}C values of the corn growth substrates (-11.7 mUr, which is typical for C_4 plants) being roughly 20 mUr less negative in their δ^{13}C values compared with the C_3 plants, pine wood (-28.0 mUr) and grass (-31.5 mUr).

The comparison of calculated δ^{13}C-CH_4 source signatures with measured bulk δ^{13}C values of the substrates shows that CH_4 emitted by both fungi is generally depleted in ^{13}C compared with the respective substrates (Fig. 4a). Based on these data, we further calculated the apparent fractionation ($\varepsilon_{app\ CH_4}$) between the δ^{13}C-CH_4 source signatures and the bulk δ^{13}C values of the growth substrates. The apparent fractionation was calculated as no metabolic pathway for the formation of CH_4 in fungi is presently known; therefore, only the initial δ^{13}C signatures of the substrates and the calculated δ^{13}C-CH_4 source signatures of the fungi can currently be compared. The values of $\varepsilon_{app\ CH_4}$ that range from -21.8 mUr (for *P. sapidus* grown on grass) to -42.2 mUr (for *L. sulphureus* grown on corn) are presented in Table 2. When grown on pine wood, $\varepsilon_{app\ CH_4}$ values are similar for *P. sapidus* (-38.4 ± 1.2 mUr) and *L. sulphureus* (-34.4 ± 0.6 mUr). The differences in $\varepsilon_{app\ CH_4}$ values between both fungal species are distinct when grown on grass (*P. sapidus*: -21.8 ± 1.7 mUr; *L. sulphureus:* $-38.6 \pm$

2.0 mUr) and corn (*P. sapidus*: -28.5 ± 2.0 mUr; *L. sulphureus*: -42.2 ± 1.1 mUr).

The calculated δ^{13}C-CO_2 source signatures of both fungi (Table 2) range from -29.0 ± 0.5 mUr (for *L. sulphureus* grown on grass) to -12.0 ± 0.3 mUr (for *P. sapidus* grown on corn). δ^{13}C-CO_2 source signatures are in a similar range for both fungi for all three substrates. However, CO_2 emitted by *L. sulphureus* is slightly more depleted in ^{13}C for all three substrates compared with *P. sapidus*. Hence, the effect of fungal species on the stable carbon isotope values of CO_2 is significant ($p = 0.008$). Moreover, the substrates used were found to influence δ^{13}C-CO_2 values significantly ($p < 0.001$).

The δ^{13}C-CO_2 source signatures of the fungi show only small deviations from the bulk δ^{13}C values of the respective substrates (Fig. 4b). However, for both fungi grown on pine wood and grass, δ^{13}C-CO_2 values are slightly less negative (a few mUr) compared with the bulk substrate. This observation is rather unexpected, as δ^{13}C-CO_2 values are usually more negative with respect to δ^{13}C values of growth substrates due to fractionation during metabolism (Bowling et al., 2008). However, when grown on corn δ^{13}C-CO_2 source signatures from both fungi are more negative compared with the substrate, and calculated $\varepsilon_{\text{app CO}_2}$ values (Table 2) are -1.1 ± 0.3 mUr and $+4.6 \pm 1.3$ mUr for *L. sulphureus* grown on corn and *P. sapidus* grown on grass respectively.

The results of the incubation experiments show that there are distinct differences in the δ^{13}C-CH_4 and δ^{13}C-CO_2 values released by both fungi. While the δ^{13}C-CO_2 source signatures are similar to the δ^{13}C values of the substrate (with $\varepsilon_{\text{app CO}_2}$ values of up to 4.6 mUr), the δ^{13}C-CH_4 source signatures deviate strongly from the respective substrate, with $\varepsilon_{\text{app CH}_4}$ values of up to -42.2 mUr. This either indicates that metabolic pathways leading to the formation of CH_4 and CO_2 have different fractionation and/or that fungal CH_4 and CO_2 are derived from different precursor compounds of the respective substrate. The growth substrates used for this study (pine wood, grass, and corn) contain distinct amounts of cellulose, hemicellulose, lignin, and other compounds in different proportions (in contrast to only using pure glucose or cellulose as the growth substrate). Hence, the δ^{13}C-CH_4 and δ^{13}C-CO_2 source signatures depend on the specific metabolic pathways used by the fungal species as well as the chemical composition of the growth substrate. The selected fungi and the growth substrates used provide a first solid basis for the potential range of δ^{13}C-CH_4 values that might occur in nature.

3.4 Fungal δ^{13}C-CH_4 values compared with known CH_4 sources

Figure 5 compares the δ^{13}C-CH_4 values emitted by fungi in relation to other known CH_4 sources in the environment that have been reported in the literature. The red bars indicate typical biogenic (formerly only considered to be produced by archaea) CH_4 sources with emissions from wetlands, ruminants, landfills, and rice paddies where δ^{13}C-CH_4 values usually range from -85 to -40 mUr. Abiotic CH_4 sources (including thermogenic or pyrolytic processes) stemming from natural gas, coal mining, and biomass burning are characterized by less negative δ^{13}C values usually ranging from -55 to -20 mUr. In addition, gas hydrates, which might be formed by both microbial and abiotic processes, cover a wide range of δ^{13}C values (-29 to -73 mUr) depending on their formation mechanisms (Kvenvolden, 1995). The δ^{13}C source signatures of plant-derived CH_4 have been reported to be in the range of -72 to -45 mUr (Keppler et al., 2006; Vigano et al., 2009) depending on their photosynthetic pathways (C_3, C_4, or CAM). Furthermore, there was a tendency towards more negative δ^{13}C-CH_4 values when the respective plant was treated with UV radiation (Vigano et al., 2009). δ^{13}C-CH_4 source signatures of humans, which might include formation by microbes in the gut as well as formation by cellular processes, show a rather wide range with values between -95 and -56 mUr (Keppler et al., 2016). The results of our experiments conducted with two fungal species and three different growth substrates provide a range of δ^{13}C-CH_4 source values from -69 to -40 mUr. This range overlaps with other eukaryotic sources, most microbial CH_4 sources, and even some abiotic CH_4 sources such as natural gas or emissions from coal mining.

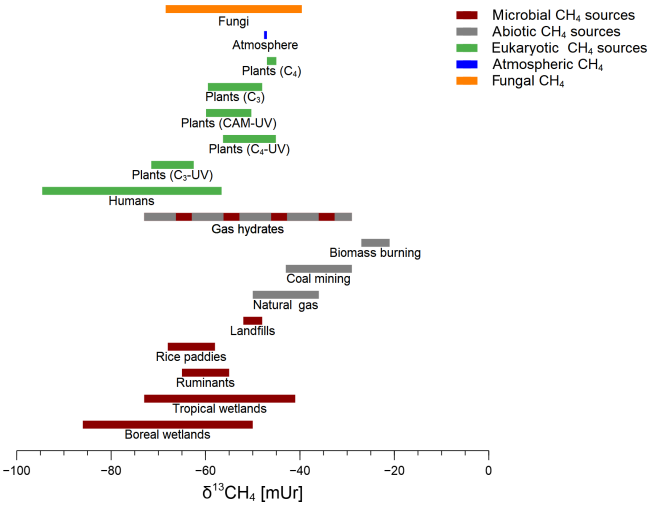

Figure 5. The range of δ^{13}C-CH_4 values of microbial CH_4 sources (red), abiotic CH_4 sources (grey), eukaryotic CH_4 sources (green), atmospheric CH_4 (blue), and fungal CH_4 from this study (orange). The red and grey dashed bar indicates a mixture of microbial and abiotic CH_4 formation processes for gas hydrates (Kvenvolden, 1995). Data were taken from Brownlow et al. (2017), Keppler et al. (2006, 2016), Kvenvolden (1995), Nisbet et al. (2016), Quay et al. (1999), and Vigano et al. (2009).

4 Conclusions

This study provided the first analysis of stable carbon isotope values of CH_4 emitted by two saprotrophic fungi that were grown on three different substrates. δ^{13}C-CH_4 and δ^{13}C-CO_2 source values were found to be dependent on the fungal species as well as the substrates decomposed by the fungi. δ^{13}C-CH_4 source values of the fungi were found to be in the range of -69 to -40 mUr and, therefore, overlap with δ^{13}C-CH_4 values reported for other CH_4 sources such as methanogenic archaea, eukaryotes, and from abiotic CH_4 sources (e.g. natural gas and coal mining). Stable carbon isotope values of CH_4 in combination with flux measurements are often applied for a better understanding of regional and global CH_4 cycling. However, in recent years it has become clear that many biogenic CH_4 sources include complex CH_4 formation processes, resulting in different isotopic fractionation patterns depending on several biochemical and abiotic factors. Thus, studying ecosystems in which more than one major CH_4 source has to be expected (e.g. methanogenic archaea, fungi, cyanobacteria, or plants) becomes increasingly complicated, as distinguishing between each individual source based solely on stable carbon isotope values might be highly challenging. Therefore, additional tools are needed to better identify the sources but also to disentangle sources and sinks. In future research, stable hydrogen isotopic values of CH_4 (δ^2H-CH_4 values) or even applications of clumped isotopes might prove to be suitable tools to better distinguish between different CH_4 sources and, thus, to better constrain the global CH_4 budget.

Data availability. The data used in this study are available from heiDATA, which is an institutional repository for research data of the Heidelberg University (https://doi.org/10.11588/data/DQYPMC, Schroll et al., 2020).

Supplement. The supplement related to this article is available online at: https://doi.org/10.5194/bg-17-3891-2020-supplement.

Author contributions. MS, KL, and FK conceived the study and designed the experiments. HZ provided fungal cultures. MS performed the experiments under the supervision of FK and KL. CE helped with gas measurements. MG measured stable isotope values of greenhouse gases. MS, FK, and KL analysed the data. MS, FK, HZ, MG, and KL discussed the results, and MS, KL and FK wrote the paper.

Competing interests. The authors declare that they have no conflict of interest.

Acknowledgements. We thank Anette Giesemann for analytical measurements of stable carbon isotope values of the bulk substrates. We are grateful to Bianka Daubertshäuser for technical support with the cultivation of the fungi and to Lukas Kohl for encouraging us to perform this study. We acknowledge financial support from the German Research Foundation (Deutsche Forschungsgemeinschaft).

Financial support. This research has been supported by the German Research Foundation (DFG grant nos. KE 884/8-2, KE 884/16-2 and LE3381/1-1).

Review statement. This paper was edited by Tina Treude and reviewed by Lukas Kohl and one anonymous referee.

References

Beckmann, S., Krüger, M., Engelen, B., Gorbushina, A. A., and Cypionka, H.: Role of bacteria, archaea and fungi involved in methane release in abandoned coal mines, Geomicrobiol. J., 28, 347–358, https://doi.org/10.1080/01490451.2010.503258, 2011.

Bižić, M., Klintzsch, T., Ionescu, D., Hindiyeh, M. Y., Günthel, M., Muro-Pastor, A. M., Eckert, W., Urich, T., Keppler, F., and Grossart, H. P.: Aquatic and terrestrial cyanobacteria produce methane, Sci. Adv., 6, eaax5343, https://doi.org/10.1126/sciadv.aax5343, 2020.

Boros, M. and Keppler, F.: Methane production and bioactivity-A link to oxido-reductive stress, Front. Physiol., 10, 1244, https://doi.org/10.3389/fphys.2019.01244, 2019.

Bowling, D. R., Pataki, D. E., and Randerson, J. T.: Carbon isotopes in terrestrial ecosystem pools and CO_2 fluxes, New Phytol., 178, 24–40, https://doi.org/10.1111/j.1469-8137.2007.02342.x, 2008.

Brand, W. A. and Coplen, T. B.: Stable isotope deltas: Tiny, yet robust signatures in nature, Isotopes Environ. Health Stud., 48, 393–409, https://doi.org/10.1080/10256016.2012.666977, 2012.

Brownlow, R., Lowry, D., Fisher, R. E., France, J. L., Lanoisellé, M., White, B., Wooster, M. J., Zhang, T., and Nisbet, E. G.: Isotopic Ratios of Tropical Methane Emissions by Atmospheric Measurement, Global Biogeochem. Cy., 31, 1408–1419, https://doi.org/10.1002/2017GB005689, 2017.

Dlugokencky, E. J., Nisbet, E. G., Fisher, R., and Lowry, D.: Global atmospheric methane: Budget, changes and dangers, Philos. T. R. Soc. A, 369, 2058–2072, https://doi.org/10.1098/rsta.2010.0341, 2011.

Ghyczy, M., Torday, C., Kaszaki, J., Szabó, A., Czóbel, M., and Boros, M.: Hypoxia-induced generation of methane in mitochondria and eukaryotic cells – An alternative approach to methanogenesis, Cell. Physiol. Biochem., 21, 251–258, https://doi.org/10.1159/000113766, 2008.

Grinhut, T., Hadar, Y., and Chen, Y.: Degradation and transformation of humic substances by saprotrophic fungi: processes and mechanisms, Fungal Biol. Rev., 21, 179–189, https://doi.org/10.1016/j.fbr.2007.09.003, 2007.

Hein, R., Crutzen, P. J., and Heimann, M.: An inverse modeling approach to investigate the global atmospheric methane cycle, Global Biogeochem. Cy., 11, 43–76, https://doi.org/10.1029/96GB03043, 1997.

Hietala, A. M., Dörsch, P., Kvaalen, H., and Solheim, H.: Carbon dioxide and methane formation in norway spruce stems infected by white-rot fungi, Forests, 6, 3304–3325, https://doi.org/10.3390/f6093304, 2015.

Keeling, C. D.: The concentration and isotopic abundances of atmospheric carbon dioxide in rural areas, Geochim. Cosmochim. Ac., 13, 322–334, https://doi.org/10.1016/0016-7037(58)90033-4, 1958.

Keppler, F., Hamilton, J. T. G., Braß, M., and Röckmann, T.: Methane emissions from terrestrial plants under aerobic conditions, Nature, 439, 187–191, https://doi.org/10.1038/nature04420, 2006.

Keppler, F., Boros, M., Frankenberg, C., Lelieveld, J., McLeod, A., Pirttilä, A. M., Röckmann, T., and Schnitzler, J. P.: Methane formation in aerobic environments, Environ. Chem., 6, 459–465, https://doi.org/10.1071/EN09137, 2009.

Keppler, F., Schiller, A., Ehehalt, R., Greule, M., Hartmann, J., and Polag, D.: Stable isotope and high precision concentration measurements confirm that all humans produce and exhale methane, J. Breath Res., 10, https://doi.org/10.1088/1752-7155/10/1/016003, 2016.

Kirschke, S., Bousquet, P., Ciais, P., Saunois, M., Canadell, J. G., Dlugokencky, E. J., Bergamaschi, P., Bergmann, D., Blake, D. R., Bruhwiler, L., Cameron-Smith, P., Castaldi, S., Chevallier, F., Feng, L., Fraser, A., Heimann, M., Hodson, E. L., Houweling, S., Josse, B., Fraser, P. J., Krummel, P. B., Lamarque, J. F., Langenfelds, R. L., Le Quéré, C., Naik, V., O'doherty, S., Palmer, P. I., Pison, I., Plummer, D., Poulter, B., Prinn, R. G., Rigby, M., Ringeval, B., Santini, M., Schmidt, M., Shindell, D. T., Simpson, I. J., Spahni, R., Steele, L. P., Strode, S. A., Sudo, K., Szopa, S., Van Der Werf, G. R., Voulgarakis, A., Van Weele, M., Weiss, R. F., Williams, J. E., and Zeng, G.: Three decades of global methane sources and sinks, Nat. Geosci., 6, 813–823, https://doi.org/10.1038/ngeo1955, 2013.

Klintzsch, T., Langer, G., Nehrke, G., Wieland, A., Lenhart, K., and Keppler, F.: Methane production by three widespread marine phytoplankton species: release rates, precursor compounds, and potential relevance for the environment, Biogeosciences, 16, 4129–4144, https://doi.org/10.5194/bg-16-4129-2019, 2019.

Kvenvolden, K. A.: A review of the geochemistry of methane in natural gas hydrate, Org. Geochem., 23, 997–1008, https://doi.org/10.1016/0146-6380(96)00002-2, 1995.

Lenhart, K., Bunge, M., Ratering, S., Neu, T. R., Schüttmann, I., Greule, M., Kammann, C., Schnell, S., Müller, C., Zorn, H., and Keppler, F.: Evidence for methane production by saprotrophic fungi, Nat. Commun., 3, https://doi.org/10.1038/ncomms2049, 2012.

Lenhart, K., Klintzsch, T., Langer, G., Nehrke, G., Bunge, M., Schnell, S., and Keppler, F.: Evidence for methane production by the marine algae Emiliania huxleyi, Biogeosciences, 13, 3163–3174, https://doi.org/10.5194/bg-13-3163-2016, 2016.

Leonowicz, A., Matuszewska, A., Luterek, J., Ziegenhagen, D., Wojtaś-Wasilewska, M., Cho, N. S., Hofrichter, M., and Rogalski, J.: Biodegradation of lignin by white rot fungi, Fungal Genet. Biol., 27, 175–185, https://doi.org/10.1006/fgbi.1999.1150, 1999.

Mikaloff Fletcher, S. E., Tans, P. P., Bruhwiler, L. M., Miller, J. B., and Heimann, M.: CH_4 sources estimated from atmospheric observations of CH_4 and its $^{13}C/^{12}C$ isotopic ratios: 1. Inverse modeling of source processes, Global Biogeochem. Cy., 18, 1–17, https://doi.org/10.1029/2004GB002223, 2004a.

Mikaloff Fletcher, S. E., Tans, P. P., Bruhwiler, L. M., Miller, J. B., and Heimann, M.: CH_4 sources estimated from atmospheric observations of CH_4 and its $^{13}C/^{12}C$ isotopic ratios: 2. Inverse modeling of CH_4 fluxes from geographical regions, Global Biogeochem. Cy., 18, 1–15, https://doi.org/10.1029/2004GB002224, 2004b.

Mukhin, V. A. and Voronin, P. Y.: Methane emission during wood fungal decomposition, Dokl. Biol. Sci., 413, 159–160, https://doi.org/10.1134/S0012496607020202, 2007.

Mukhin, V. A. and Voronin, P. Y.: A new source of methane in boreal forests, Appl. Biochem. Microbiol., 44, 297–299, https://doi.org/10.1134/S0003683808030125, 2008.

Naik, V., Voulgarakis, A., Fiore, A. M., Horowitz, L. W., Lamarque, J.-F., Lin, M., Prather, M. J., Young, P. J., Bergmann, D., Cameron-Smith, P. J., Cionni, I., Collins, W. J., Dalsøren, S. B., Doherty, R., Eyring, V., Faluvegi, G., Folberth, G. A., Josse, B., Lee, Y. H., MacKenzie, I. A., Nagashima, T., van Noije, T. P. C., Plummer, D. A., Righi, M., Rumbold, S. T., Skeie, R., Shindell, D. T., Stevenson, D. S., Strode, S., Sudo, K., Szopa, S., and Zeng, G.: Preindustrial to present-day changes in tropospheric hydroxyl radical and methane lifetime from the Atmospheric Chemistry and Climate Model Intercomparison Project (ACCMIP), Atmos. Chem. Phys., 13, 5277–5298, https://doi.org/10.5194/acp-13-5277-2013, 2013.

Nisbet, E. G., Dlugokencky, E. J., Manning, M. R., Lowry, D., Fisher, R. E., France, J. L., Michel, S. E., Miller, J. B., White, J. W. C., Vaughn, B., Bousquet, P., Pyle, J. A., Warwick, N. J., Cain, M., Brownlow, R., Zazzeri, G., Lanoisellé, M., Manning, A. C., Gloor, E., Worthy, D. E. J., Brunke, E. G., Labuschagne, C., Wolff, E. W., and Ganesan, A. L.: Rising atmospheric methane: 2007–2014 growth and isotopic shift, Global Biogeochem. Cy., 30, 1356–1370, https://doi.org/10.1002/2016GB005406, 2016.

Pataki, D. E., Ehleringer, J. R., Flanagan, L. B., Yakir, D., Bowling, D. R., Still, C. J., Buchmann, N., Kaplan, J. O., and Berry, J. A.: The application and interpretation of Keeling plots in terrestrial carbon cycle research, Global Biogeochem. Cy., 17, 1022, https://doi.org/10.1029/2001GB001850, 2003.

Paul, D., Skrzypek, G., and Fórizs, I.: Normalization of measured stable isotopic compositions to isotope reference scales – a review, Rapid Commun. Mass Spectrom., 21, 3006–3014, https://doi.org/10.1002/rcm.3185, 2007.

Prather, M. J., Holmes, C. D., and Hsu, J.: Reactive greenhouse gas scenarios: Systematic exploration of uncertainties and the role of atmospheric chemistry, Geophys. Res. Lett., 39, L09803, https://doi.org/10.1029/2012GL051440, 2012.

Quay, P., Stutsman, J., Wilbur, D., Snover, A., Dlugokencky, E., and Brown, T.: The isotopic composition of atmospheric methane, Global Biogeochem. Cy., 13, 445–461, https://doi.org/10.1029/1998GB900006, 1999.

Ralph, J. P. and Catcheside, D. E. A.: Biodegradation by White-Rot Fungi, in: Industrial Applications, Springer Berlin Heidelberg, 303–326, 2002.

Saunois, M., Bousquet, P., Poulter, B., Peregon, A., Ciais, P., Canadell, J. G., Dlugokencky, E. J., Etiope, G., Bastviken, D., Houweling, S., Janssens-Maenhout, G., Tubiello, F. N., Castaldi, S., Jackson, R. B., Alexe, M., Arora, V. K., Beerling, D. J., Bergamaschi, P., Blake, D. R., Brailsford, G., Brovkin, V., Bruhwiler,

L., Crevoisier, C., Crill, P., Covey, K., Curry, C., Frankenberg, C., Gedney, N., Höglund-Isaksson, L., Ishizawa, M., Ito, A., Joos, F., Kim, H.-S., Kleinen, T., Krummel, P., Lamarque, J.-F., Langenfelds, R., Locatelli, R., Machida, T., Maksyutov, S., McDonald, K. C., Marshall, J., Melton, J. R., Morino, I., Naik, V., O'Doherty, S., Parmentier, F.-J. W., Patra, P. K., Peng, C., Peng, S., Peters, G. P., Pison, I., Prigent, C., Prinn, R., Ramonet, M., Riley, W. J., Saito, M., Santini, M., Schroeder, R., Simpson, I. J., Spahni, R., Steele, P., Takizawa, A., Thornton, B. F., Tian, H., Tohjima, Y., Viovy, N., Voulgarakis, A., van Weele, M., van der Werf, G. R., Weiss, R., Wiedinmyer, C., Wilton, D. J., Wiltshire, A., Worthy, D., Wunch, D., Xu, X., Yoshida, Y., Zhang, B., Zhang, Z., and Zhu, Q.: The global methane budget 2000–2012, Earth Syst. Sci. Data, 8, 697–751, https://doi.org/10.5194/essd-8-697-2016, 2016.

Saunois, M., Stavert, A. R., Poulter, B., Bousquet, P., Canadell, J. G., Jackson, R. B., Raymond, P. A., Dlugokencky, E. J., Houweling, S., Patra, P. K., Ciais, P., Arora, V. K., Bastviken, D., Bergamaschi, P., Blake, D. R., Brailsford, G., Bruhwiler, L., Carlson, K. M., Carrol, M., Castaldi, S., Chandra, N., Crevoisier, C., Crill, P. M., Covey, K., Curry, C. L., Etiope, G., Frankenberg, C., Gedney, N., Hegglin, M. I., Höglund-Isaksson, L., Hugelius, G., Ishizawa, M., Ito, A., Janssens-Maenhout, G., Jensen, K. M., Joos, F., Kleinen, T., Krummel, P. B., Langenfelds, R. L., Laruelle, G. G., Liu, L., Machida, T., Maksyutov, S., McDonald, K. C., McNorton, J., Miller, P. A., Melton, J. R., Morino, I., Müller, J., Murguia-Flores, F., Naik, V., Niwa, Y., Noce, S., O'Doherty, S., Parker, R. J., Peng, C., Peng, S., Peters, G. P., Prigent, C., Prinn, R., Ramonet, M., Regnier, P., Riley, W. J., Rosentreter, J. A., Segers, A., Simpson, I. J., Shi, H., Smith, S. J., Steele, L. P., Thornton, B. F., Tian, H., Tohjima, Y., Tubiello, F. N., Tsuruta, A., Viovy, N., Voulgarakis, A., Weber, T. S., van Weele, M., van der Werf, G. R., Weiss, R. F., Worthy, D., Wunch, D., Yin, Y., Yoshida, Y., Zhang, W., Zhang, Z., Zhao, Y., Zheng, B., Zhu, Q., Zhu, Q., and Zhuang, Q.: The Global Methane Budget 2000–2017, Earth Syst. Sci. Data, 12, 1561–1623, https://doi.org/10.5194/essd-12-1561-2020, 2020.

Schroll, M., Keppler, F., Greule, M., Eckhardt, C., Zorn, H., and Lenhart, K.: The stable carbon isotope signature of methane produced by saprotrophic fungi [Dataset], https://doi.org/10.11588/data/DQYPMC, 2020.

Ten Have, R. and Teunissen, P. J. M.: Oxidative mechanisms involved in lignin degradation by white-rot fungi, Chem. Rev., 101, 3397–3413, https://doi.org/10.1021/cr000115l, 2001.

Tyler, S. C.: Stable carbon isotope ratios in atmospheric methane and some of its sources, J. Geophys. Res., 91, 13232, https://doi.org/10.1029/jd091id12p13232, 1986.

Valášková, V. and Baldrian, P.: Degradation of cellulose and hemicelluloses by the brown rot fungus *Piptoporus betulinus* – Production of extracellular enzymes and characterization of the major cellulases, Microbiology, 152, 3613–3622, https://doi.org/10.1099/mic.0.29149-0, 2006.

Vigano, I., Röckmann, T., Holzinger, R., van Dijk, A., Keppler, F., Greule, M., Brand, W. A., Geilmann, H., and van Weelden, H.: The stable isotope signature of methane emitted from plant material under UV irradiation, Atmos. Environ., 43, 5637–5646, https://doi.org/10.1016/j.atmosenv.2009.07.046, 2009.

Voulgarakis, A., Naik, V., Lamarque, J.-F., Shindell, D. T., Young, P. J., Prather, M. J., Wild, O., Field, R. D., Bergmann, D., Cameron-Smith, P., Cionni, I., Collins, W. J., Dalsøren, S. B., Doherty, R. M., Eyring, V., Faluvegi, G., Folberth, G. A., Horowitz, L. W., Josse, B., MacKenzie, I. A., Nagashima, T., Plummer, D. A., Righi, M., Rumbold, S. T., Stevenson, D. S., Strode, S. A., Sudo, K., Szopa, S., and Zeng, G.: Analysis of present day and future OH and methane lifetime in the ACCMIP simulations, Atmos. Chem. Phys., 13, 2563–2587, https://doi.org/10.5194/acp-13-2563-2013, 2013.

Whiticar, M. J.: Stable Isotopes and Global Budgets, in: Atmospheric Methane: Sources, Sinks, and Role in Global Change, Springer Berlin Heidelberg, 138–167, 1993.

Whiticar, M. J.: Carbon and hydrogen isotope systematics of bacterial formation and oxidation of methane, Chem. Geol., 161, 291–314, https://doi.org/10.1016/S0009-2541(99)00092-3, 1999.

Wishkerman, A., Greiner, S., Ghyczy, M., Boros, M., Rausch, T., Lenhart, K., and Keppler, F.: Enhanced formation of methane in plant cell cultures by inhibition of cytochrome c oxidase, Plant Cell Environ., 34, 457–464, https://doi.org/10.1111/j.1365-3040.2010.02255.x, 2011.